Low energy Ar ion milling of FIB TEM specimens from 14 nm and future FinFET technologies

C.S. Bonifacio, P. Nowakowski, M.J. Campin, M.L. Ray and P.E. Fischione
E.A. Fischione Instruments, Inc., Export, PA 15632 USA

Abstract

Transmission electron microscopy (TEM) specimens are typically prepared using the focused ion beam (FIB) due to its site specificity, and fast and accurate thinning capabilities. However, TEM and high-resolution TEM (HRTEM) analysis may be limited due to the resulting FIB-induced artifacts. This work identifies FIB artifacts and presents the use of argon ion milling for the removal of FIB-induced damage for reproducible TEM specimen preparation of current and future fin field effect transistor (FinFET) technologies. Subsequently, high-quality and electron-transparent TEM specimens of less than 20 nm are obtained.

Introduction

Today's semiconductor devices, including FinFETs, are complex due to the multigate transistors and three-dimensional gate structure design. The advanced devices are at the 10 nm node and 7 nm node, with the later at the ramping stage of production [1]. At the 10 nm node, the source-drain channel or "fins" are 25% taller and 25% more closely spaced than the 14 nm node technology [2].

Currently, metrology and physical failure analysis are challenging due to the high-aspect ratio and complexity of the FinFET structure. To accurately measure the structure of these devices, TEM is indispensable due to the resolution it provides. TEM characterization is part of the workflow in semiconductor process development and integration, and failure analysis for critical dimension (CD) measurements. Therefore, TEM is critical for the development and production of advanced semiconductor devices given the decreasing device size.

Specimen thickness of 20 nm or less is required to characterize the 3D structures of 14 nm node FinFET gate oxide in the TEM [3]. Consequently, fast and reproducible TEM specimen preparation is essential. TEM specimens are usually prepared using a FIB due to the site specificity and accuracy of specimen thinning and extraction that it provides [4, 5]. However, Ga^+ milling causes artifacts such as surface amorphization and ion-implanted layers, which subsequently limits analytical and high-resolution electron microscopy. In this work, we present targeted, small spot (< 1 μm), low energy (< 1 kV) Ar^+ milling for reproducible specimen preparation of advanced devices with specimen thicknesses of less than 20 nm without FIB-induced artifacts.

Discussion

Sample preparation

A Broadwell M core processor [Intel] with 14 nm FinFET structure was depackaged and from it a cross-section specimen was created in the FIB at 30 kV using the inverted method [6]. During the FIB milling process, additional steps were performed to maintain specimen integrity during the polishing steps and to prevent Ga redeposition onto the specimen: by milling the top metal lines (Figure 1a-b) and milling the original bottom portion of the Si substrate (Figure 1d).
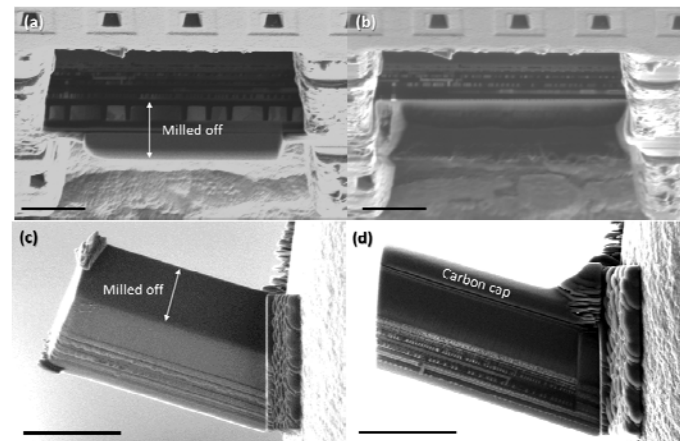
Figure 1: FIB images from the additional steps before and after removing the top metal lines (a-b) and the initial bottom portion of the Si substrate (c-d) performed during the inverted FIB specimen preparation. Scale bar is 5 μm.

The FinFET structures were targeted during FIB milling by imaging at a low accelerating voltage of 2 kV; a secondary electron detector was used to image the fin structure in between the polishing steps. Specimen thickness ranging from 100 to 50 nm was achieved after 5 kV polishing in the FIB.

FIB-induced damage and its removal

The damage on the specimen induced by the FIB comprises amorphous damage and a Ga-implanted layer. Numerous studies have shown a direct relationship between amorphous damage layer thickness and accelerating FIB voltage, e.g., a 30 kV FIB beam causes 20 to 30 nm [7] while 5 kV FIB beam

causes 2.5 nm of amorphous damage [8] on Si. Conversely, very few studies [9][10] have measured the Ga implanted layer after FIB milling.

Therefore, we investigated both amorphous damage and Ga-implanted layers from FIB milling. To simplify the analysis, a crystalline Si specimen (instead of a FinFET specimen) was analyzed. The results show that post-FIB cleaning using low energy, concentrated beam, Ar^+ milling creates TEM specimens free from Ga FIB-induced damage. This ion mill operates at low energy (< 1 kV) and concentrated beam (< 1 µm) with the argon ions rastered across the FIB specimen.

The thickness of the amorphous damage from FIB milling was investigated by creating a FIB specimen based on van Leer et al. [11]. Using the same methodology, the Si specimen milled at 30 kV using Ga FIB was further milled using the Ar milling system at 900 eV. The two areas of the Si specimen were cross sectioned using the FIB to create a TEM lamella exposing the sidewall areas from the 30 kV FIB milling and the 30 kV FIB milling/900 eV Ar^+ milling (Figure 2a-b). A 23 nm amorphous layer on the Si specimen was observed after 30 kV FIB milling (Figure 2a). This amorphous layer was completely removed after 900 eV argon milling (Figure 2b). Based on these results, it is expected that the thinner amorphous damage of 2.5 nm in Si [8] from specimen prepared using 30 kV followed by 5 kV polishing step in the FIB will be completely removed by argon ion milling at 900 eV.
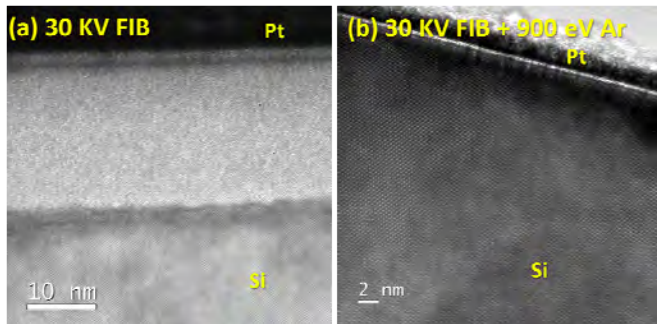

Figure 2: TEM images of the sidewall areas of a Si specimen milled using 30 kV FIB (a) and 30 kV FIB followed by 900 eV argon ion milling.

The thickness of Ga-implanted layers was quantified by X-ray characteristic emission measurement generated by the electron beam in the specimen by energy dispersive X-ray spectroscopy (EDS). The thickness of implanted Ga after FIB milling was determined using the XPP model [12][13], which determines the correlation between layer thickness and k-ratios measured by EDS. This technique has been widely used for thickness determination in the scanning electron microscope (SEM) [14][15][16]. The model is implemented in LayerProbe software [Oxford Instruments] used for EDS acquisition.

The EDS spectra acquired after gallium FIB milling and argon ion milling (Figure 3) show the reduction of the Ga signal after 5 kV in comparison to 30 kV FIB milling alone and no Ga signal detected after 300 eV Ar milling. The Si specimen thickness and the Ga-implanted layers after FIB milling versus after FIB milling plus argon milling were measured and are shown in Table 1. The measured Ga-implanted layer thickness after 30 kV FIB milling in Table 1 correlates to Ishitani et al. [9] results of < 10 nm of Ga layer, which validates our XPP model-derived results.
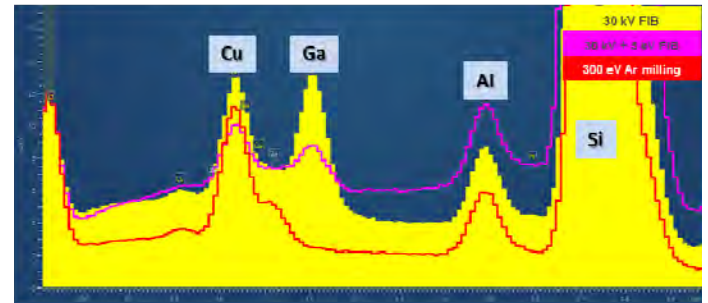

Figure 3: Comparison of EDS spectra from Si specimen milled using the gallium FIB and the PicoMill argon ion milling system. Si specimen milled in the FIB at 30 kV (yellow); in the FIB at 30 kV followed by 5 kV (pink); and in the FIB at 30 kV followed by 5 kV plus in the Ar^+ mill at 300 eV (red).

Table 1- Calculated Si specimen thickness and Ga-implanted layer thickness after Ga FIB and Ar^+ milling.

	Si Thickness [nm]	Ga-implanted layer per side [nm]
30 kV Ga FIB	100	1.5 ± 0.1
30 kV, then 5 kV Ga FIB	130	0.3 ± 0.08
500 eV, then 300 eV Ar^+ milling post-FIB	70	0

Iterative ion milling

The PicoMill® TEM specimen preparation system [Fischione Instruments] with a 600 nm diameter argon ion beam was used for final polishing of FIB specimens. The system includes a LaB_6 electron source and electron detectors – a secondary electron detector (SED) and a scanning transmission electron microscope (STEM) – that provide in situ imaging during ion milling. The FIB specimen is mounted on a specimen holder that is compatible with both the PicoMill system and the TEM.

The concentrated beam of argon ions is rastered and directed toward the leading edge of the sample, which in this case is the Si substrate (Figure 4). The change in contrast after milling in the SED (Figure 4a and 4c) and STEM (Figure 4b and d) images on the Si substrate were an indication of the reduction in specimen thickness.
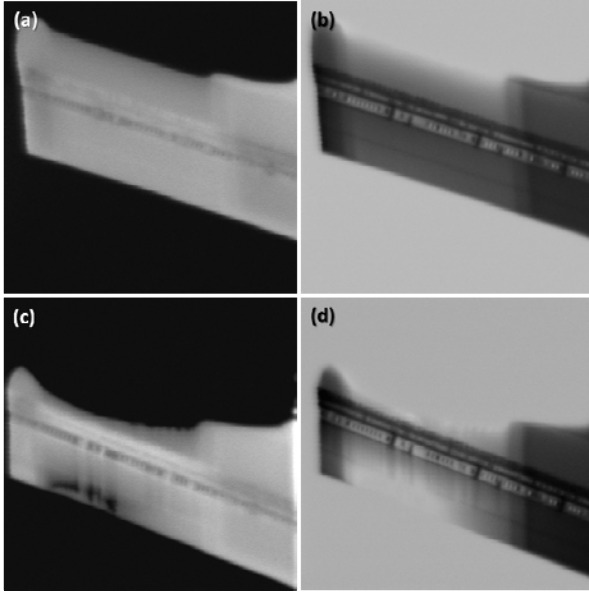
Figure 4: SED and STEM images in the ion milling system acquired before (a-b) and after (c-d) milling.

Before ion milling, a high-angle annular dark field scanning transmission electron microscopy (HAADF-STEM) image was acquired with the specimen tilted at ± 27°. This was performed to determine the position and number of fins across the TEM specimen. It is imperative to note the side of the specimen milled with respect to the layers observed in the STEM images. In this case, the fin structure is the area of interest. The same methodology can be applied when targeting a specific integrated circuit (IC) feature or possibly a defect.

Figure 5a shows three fin structures before argon ion milling; in between the fins are metal layers, specifically metal/fin/metal/fin/metal/fin (labelled as M/F/M/F/M/F in Figure 5a), from bottom to top in the image. Ion milling one side of the specimen at a 10° tilt using 700 eV beam energy for 15 minutes resulted in two metal and two fin layers (M/F/M/F), as shown in Figure 5b. Ion milling of the same side of the specimen at a 10° tilt using 500 eV beam energy for 20 minutes left only a portion of metal layer and one fin [M/F], as shown in Figure 5c. The fin structure (F) comprised the gate oxide, measured with Gate length,$_{14\ nm\ node}$ = 20 nm [17]. Also, the F/M/F layers are two gates apart with the measured distance of Gate pitch,$_{14\ nm\ node}$ = 70 nm [1]. At the completion of ion milling, the specimen thickness of the M/F can be estimated to at least 20 nm. The fin structure, as well as some of the metal layer, is shown in Figure 5c.

The 700 eV and 500 eV milling steps removed the metal and gate oxide over the fin structure. The milling rate at 700 eV is estimated as 10 min./layer of metal and 5 min./layer of gate oxide. Such results made sense given that the metal layers are comprised of W, which has a lower sputtering rate than the silicon oxide of the fin layer. Longer milling times at lower energy are to be expected at 500 eV, i.e., the milling rates of < 10 min./layer of metal and < 5 min./layer of gate oxide.
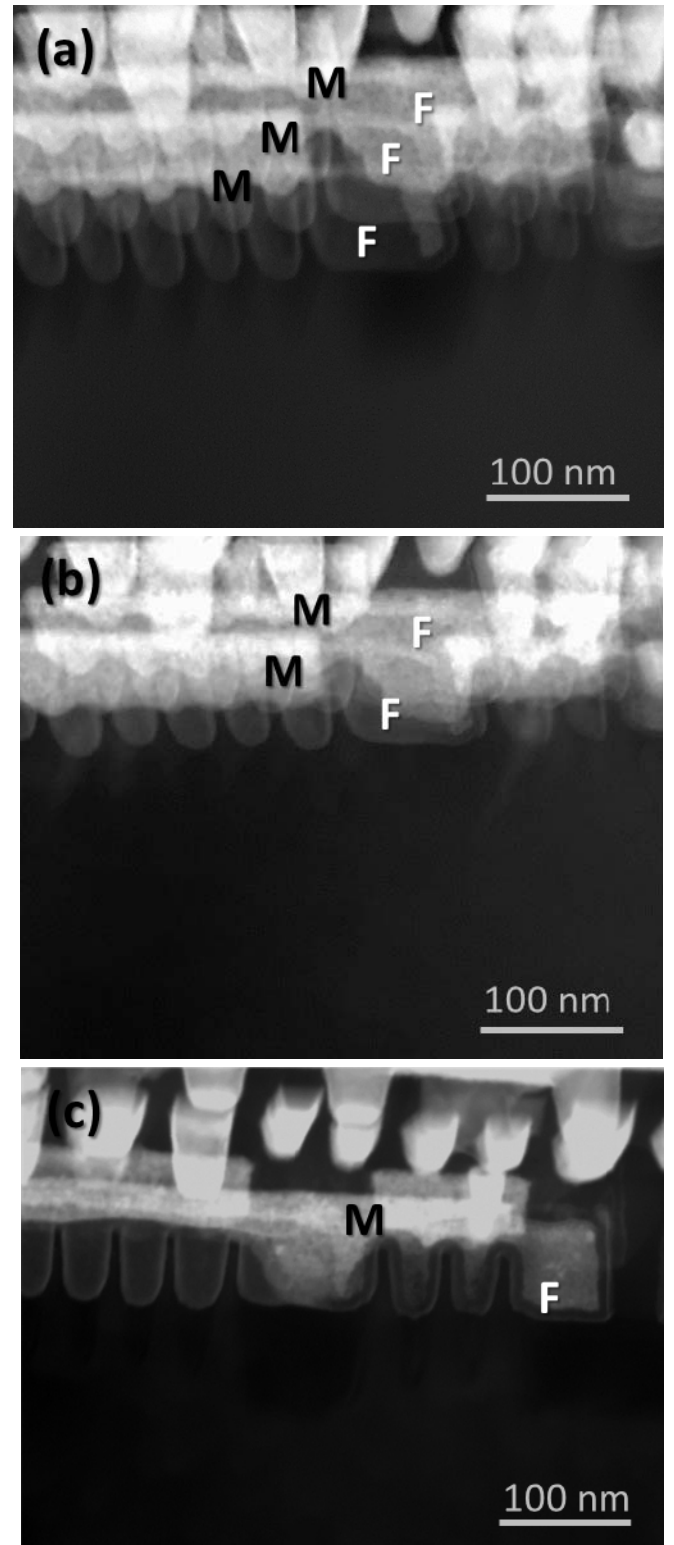

Figure 5: HAADF-STEM images of the specimen tilted at +27° before (a) and after milling at 700 eV (b) and 500 eV (c). M and F indicate the metal (M) and the fin (F) layers.

TEM images acquired between milling steps at decreasing energies displayed the transition from the epitaxial source/drain (S/D) after 700 eV into the metal gate structure of the FinFET after 500 eV milling (Figure 6a). The disappearance of the W intermetallic layer and SiGe S/D from 700 eV to 500 eV (Figure 6b) indicates controlled milling, which allows for the targeting of specific IC features.
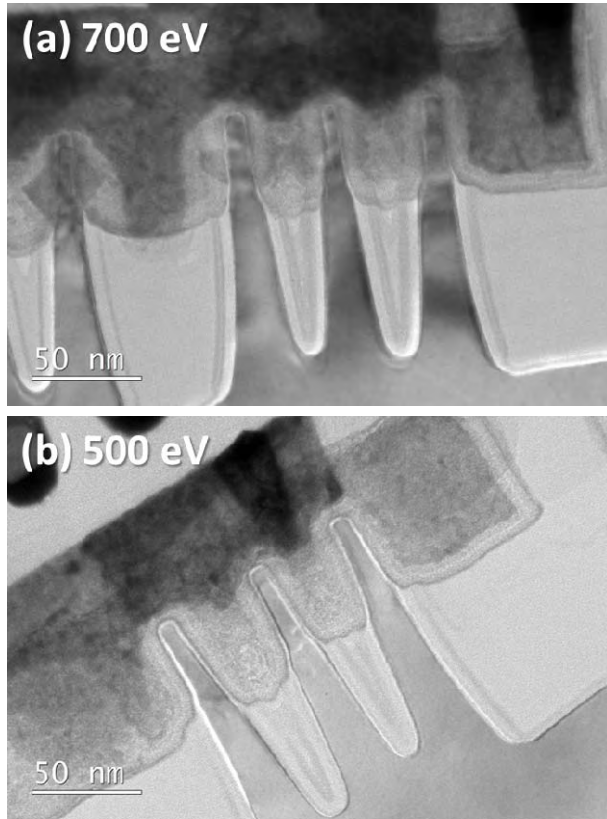

Figure 6: TEM images after 700 eV (a) and 500 eV (b) milling show the ability to precisely control the progression of milling through the fin structure.

High-quality TEM specimens

To compare the quality of the TEM specimens, an aberration-corrected JEM-ARM200F TEM [JEOL] in STEM mode was operated at 200 kV to image the TEM specimen after Ga$^+$ FIB milling and after Ar$^+$ milling. Figure 7 are atomic-resolution dark field STEM images after Ga$^+$ FIB milling and Ar$^+$ milling that show electron-transparent specimens of differing specimen quality. Low magnification images after Ga$^+$ FIB milling show that the FinFET was decorated by particles (Figure 7a) while the Ar$^+$ milled specimen was of significantly better quality (Figure 7b). The Si atoms on the fin in Figure 7c are unclear due to the bright haze over the surface, which may be FIB-induced damage. The fast Fourier transform acquired from the Si in the fin (Figure 7c, inset) shows diffused halo in the background, which typically originates from an amorphous material; therefore, the specimen has an amorphous surface from FIB milling. However, the Ar$^+$ milled specimen in Figure 7d has an amorphous-free surface (Figure 7d, inset) and clearly shows individual atoms of Si on the fin

and amorphous high-k and work-function material above the fin.

The thickness of the Ar$^+$ milled specimen used for the atomic resolution imaging was determined using electron energy loss spectroscopy (EELS). The energy-filtered TEM (EFTEM) thickness map is a relative-thickness calculated map based on the ratio of the zero-loss map (not shown) and the unfiltered image (Figure 8a) using the log-ratio method [18]. The relative thickness map is in units of t/λ, where t is the specimen thickness and λ is the inelastic mean free path of the primary beam electrons through a material at a given accelerating voltage. Figure 8a and b show an unfiltered image and an associated EFTEM thickness map of the Ar$^+$ milled specimen.

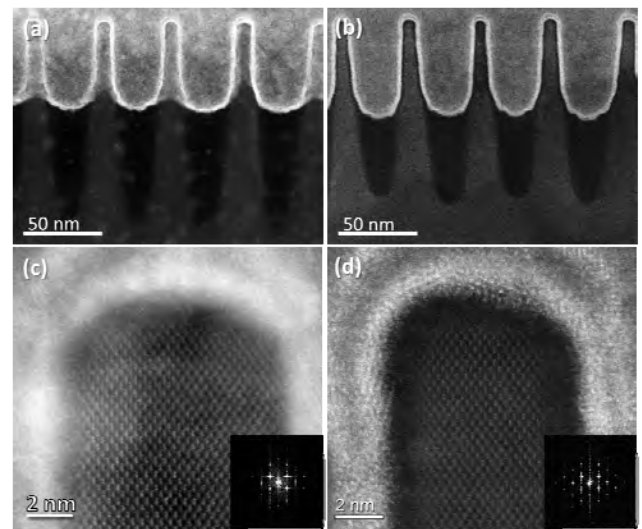*Figure 7: HAADF-STEM images of FinFET specimen Ga$^+$ FIB milled at 30 kV, followed by 5 kV (a and c). Compare to a similarly prepared FinFET specimen that was Ar$^+$ ion milled at 700 eV, 500 eV (b), and 300 eV (d) following FIB preparation. Insets in (c) and (d) are FFT derived from the Si in the fin.*
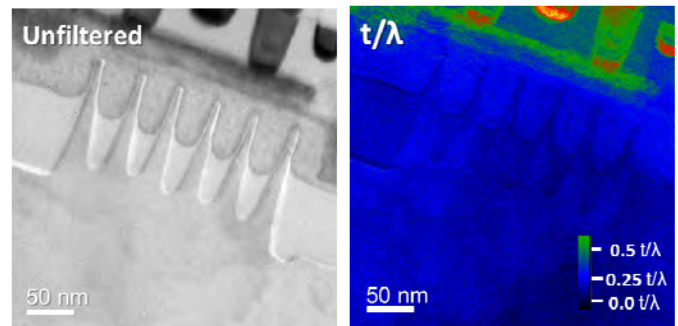

Figure 8: Unfiltered image (a) and EELS thickness map (b) of the Ar$^+$ milled specimen in Figure 7b. The color is based on the t/λ scale.

Table 2 shows the thickness values calculated from the relative t/λ values, which are based on a value of λ for Si with 300 keV primary electrons.

Table 2: Calculated specimen thickness, t, given the measured t/λ and mean-free path (MFP) value of 174.298 nm [19] for crystalline Si at 300 kV accelerating voltage.

	t/λ	Thickness, t [nm]
Si fin	0.11	19.2
Si substrate	0.07	12.2

The thinnest part of the specimen was at the Si substrate and at the FinFET structure based on the dark blue color ($t/\lambda = 0.25$) of these areas in comparison to the metal layers in green ($t/\lambda = 0.5$) of the EFTEM map in Figure 8. The area of the fins was $t/\lambda = 0.11$, which is 19.2 nm, while the Si substrate was $t/\lambda = 0.07$, which is 12.2 nm. The resulting thickness using targeted Ar^+ milling surpasses the specimen thickness requirement of 20-30 nm for imaging 14 nm FinFET structure [3]. Furthermore, the measured thickness at the fin of 19.2 nm is close to the initially estimated specimen thickness of at least 20 nm based the STEM image in Figure 5c.

Outlook and Conclusions

This work investigates 14 nm FinFET technology but is applicable for 10 and 7 nm FinFET technologies that are currently in production. Using the reported gate pitch and gate length for the 14 nm and 10 nm Intel FinFET devices, the milling rates for 700 eV post-FIB clean-up of the fin structure with the gate oxide and metal layers can be estimated and are summarized in Table 3.

Table 3: Ar^+ milling rates in the PicoMill ion milling system of current Intel FinFET technologies at 700 eV and 10° specimen tilt.

	14 nm node	10 nm node
Fin layer	4.0 nm/min.	3.6 nm/min.
Metal layer	3.0 nm/min.	1.8 nm/min.

Gate length,14 nm node = 20 nm [17] Gate pitch,14 nm node = 70 nm [2]
Gate length,10 nm node = 18 nm [20] Gate pitch,10 nm node = 54 nm [2]

The decreasing gate pitch of future FinFET technologies will make targeting the fin structure challenging. Targeted milling is necessary – from FIB preparation to post-FIB clean-up using Ar^+ milling. Based on our results, FIB preparation of three to five fin structures, followed by iterative argon ion milling to target one fin structure, results in a specimen thickness of less than the gate length of device, i.e., < 20 nm for 14 nm node and < 18 nm for 10 nm node. Therefore, specimen preparation that results in a TEM specimen thickness of 12 to 19 nm is adequate to prepare a 10 nm FinFET.

Sample preparation of 14 nm FinFET TEM specimens using a concentrated argon beam without FIB-induced damage was demonstrated. High-quality specimens for analytical and high-resolution electron microscopy analysis were obtained. Reproducible specimen preparation with exceptional specimen thickness, less than 20 nm, for imaging and analysis of FinFET structures is possible.

Acknowledgment

References

[1] M Lapedus, Semiconductor Engineering (2018), https://semiengineering.com/nodes-vs-node-lets/

[2] Bohr, M.., "Leading at the Edge: Intel Technology and Manufacturing," *Technology and Manufacturing Day*, San Francisco, CA, March 2017.

[3] Feng, H., Low, G.R., Tan, P.K., Zhao, Y.Z., Yap, H.H., Dawood, M.K., Zhou, Y., Du, A.Y., Chen, C.Q., Tan, H., Huang, Y.M., Wang, D.D., Lam, J., Mai, Z.H.., "Investigation of Protection Layer Materials for Ex-situ 'Lift-Out' TEM Sample Preparation with FIB for 14 nm FinFET," *Proc 40th Int'l Symp for Testing and Failure Analysis*, Houston, TX, November 2014, pp. 478-482.

[4] Mayer, J., Giannuzzi, L.A., Kamino, T. and Michael, J., "TEM Sample Preparation and FIB-induced Damage," *MRS Bulletin*, Vol. 32, (2007), pp. 400-407.

[5] Giannuzzi, L.A., and Stevie, F.A., "A review of focused ion beam milling techniques for TEM specimen preparation," *Micron*, Vol. 30, (1999), pp. 197-204.

[6] Alvis, R., Blackwood, J., Lee, S-H., Bray, M., "High-throughput, site-specific sample prep of ultra-thin TEM lamella for process metrology and failure analysis," *Proc 38th Int'l Symp for Testing and Failure Analysis*, Phoenix, AZ, November 2012, pp. 391-398

[7] Kato, N.I., "Reducing focused ion beam damage to transmission electron microscopy samples." *J, Electron Microsc.* Vol. 53.5, (2004), 451-458.

[8] Mayer, J., Giannuzzi, L.A., Kamino, T. and Joseph Michael. "TEM sample preparation and FIB-induced damage." *MRS bulletin* 32, (2007):pp. 400-407.

[9] Ishitani, T., H. Koike, T. Yaguchi, and T. Kamino. "Implanted gallium-ion concentrations of focused-ion-beam prepared cross sections." *J. Vac. Sci. Technol. B,* Vol. 16, (1998), pp. 1907-1913.

[10] Nowakowski, P., Bonifacio, C.S., Campin, M.J., Ray, M.L., and Fischione, P.E., "Accurate removal of implanted gallium and amorphous damage from TEM specimens after focused ion beam (FIB) preparation,"

Microsc Microanal, Vol. 23 (Suppl 1), (2017), pp. 300-301.

[11] van Leer, B., Genc, A., & Passey, R. (2017). "Ga$^+$ and Xe$^+$ FIB milling and measurement of FIB damage in aluminum," *Microscopy and Microanalysis, Microsc Microanal,* Vol. 23 (Suppl 1), (2017), pp. 296-297.

[12] Pouchou, J.L., Pichoir F.," X-ray microanalysis of stratified specimens," *Anal Chim Acta*, Vol. 283, (1993), pp. 81–97.

[13] Pouchou, J.L., Pichoir F., "Electron probe X-ray microanalysis applied to thin surface films and stratified specimens," *Scanning Microsc Suppl* , Vol. 7, (1993), pp. 167–89.

[14] Nowakowski, P., Christien, F., Allart, M. Borjon-Piron, Y., Le Gall, R. "Measuring grain boundary segregation using wavelength dispersive X-ray spectroscopy: Further developments," *Surface Science,* Vol. 605, (2011), pp. 848-585.

[15] Hiscock, M., Dawson, M., Lang, C., Hartfield, C., Statham, P., "In-Situ Quantification of TEM Lamella Thickness and Ga Implantation in the FIB," *Microsc Microanal*, Vol. 20 (Suppl 3), 2014, pp.342-343.

[16] Christien, F., Ferchaud, E., Nowakowski, P., Allart, M. Use of Electron Probe MicroAnalysis to Determine the Thickness of Thin Films in Materials Science, X-Ray Spectroscopy, Dr. Shatendra K Sharma (Ed.), *InTech* (2012), pp.101-118.

[17] 14 nm Lithography Process (2018), https://en.wikichip.org/wiki/14_nm_lithography_process

[18] Egerton, R. F., *Electron energy-loss spectroscopy in the electron microscope 3rd edition*, Springer (New York, 2011).

[19] Iakoubovskii, K., Mitsuishi, K., Nakayama, Y. and Furuya, K., "Thickness measurements with electron energy loss spectroscopy," *Microsc Res and Tech*, Vol. 71, (2008), pp. 626–631.

[20] S. Jones, IEDM 2017- Intel versus GLOBALFOUNDRIES at the leading edge (2018), https://www.semiwiki.com/forum/content/7191-iedm-2017-intel-versus-globalfoundries-leading-edge.html